Wei et al. EURASIP Journal on Advances in Signal Processing 2012, 2012:246
http://asp.eurasipjournals.com/content/2012/1/246

EURASIP Journal on Advances in Signal Processing
a SpringerOpen Journal

RESEARCH Open Access

Ionospheric decontamination for skywave OTH radar based on complex energy detector

You Wei*, He Zishu and Wang Shuangling

Abstract

For over-the-horizon (OTH) radar, the ocean clutter is very strong. And this becomes a big challenge for the target detection. The clutter suppression is a very important procedure for the OTH radar. For the skywave OTH radar, the radar signal will propagate through the ionosphere. This will cause a contamination due to its unstable movement. Then the Bragg frequencies will be smeared and clutter spectrum will spread wider rather than a single line spectra. This smear will cause the target more difficult to be detected and even buried in clutter. Compensation is necessary to cancel the ionospheric effect. This article proposes the clutter decontamination algorithm based on the complex energy detector (CED). The energy detector (ED) is originally proposed to demodulate the real AM–FM signals. The ED is expanded to complex domain. After the expansion, there is no mutual coupling between the amplitude and frequency component for an AM–FM signal. The phase of the Bragg clutter return contaminated by the ionosphere is modeled by a frequency-modulated signal, while its magnitude is amplitude modulated. The CED algorithm is applied to track the instantaneous frequency of the contaminated return signal, which is then used for compensation. Simulation results are presented. The simulation results show that, comparing with the Hankel rank reduction algorithm, the proposed algorithm has better performance under the situation of large frequency fluctuation.

Keywords: Skywave OTH radar, Ionospheric decontamination, Complex energy detector (CED)

1. Introduction

The skywave over-the-horizon (OTH) radar works in HF band, and can see over 3000-km long distance. It has the advantages over other radars to see over the horizon and longer radar range. This feature is achieved by using the skywave propagation. Detecting ships and aircrafts over the sea surface is an important task for OTH radar. The targets often can be masked by the ocean clutter. It has been observed that if the sea surface is illuminated by HF waves, then significant energy at a defined frequency shift can be received. The frequency shift is referred to as Bragg lines, and has a close relation with the radar frequency defined by [1]

$$f_b = \pm\sqrt{\frac{gf_c}{\pi c}} \tag{1}$$

where g is the acceleration due to gravity, and f_c is the radar frequency, c is the speed of light.

The ocean clutter signal is very strong and can conceal the target if it is moving slowly, target detection would fail. For a skywave radar case, this problem is even more serious as the clutter signal may be contaminated by the ionosphere path or wind over the ocean surface. The ionosphere is typically multi-layered and there are generally multiple ionospheric propagation paths to and from targets and clutter sources. Radar performance can degrade when one of the ionospheric propagation paths is so distorted as to reduce the spectral isolation between scatter of the transmitted waveform [2]. This contamination or distortion can cause the first-order Bragg lines shift near the theoretical frequency in Equation (1). This smearing can lead the clutter spectrum spans more widely in frequency domain and masks the targets. The performance of OTHR strongly depends on the radar frequency and it is time varying. Although the frequency management systems can adaptively select a proper frequency for the OTH radar, it can only partially eliminate the ionospheric effect, and thus it is not possible to totally avoid

* Correspondence: yoyouv@163.com
Department of Electronic Engineering, University of Electronic Science and Technology of China, Chengdu 611731, China

the smearing [3-5]. So, the clutter contamination is still an important factor to be considered. To detect the targets under the contaminated clutter environment, the clutter should be corrected first. The instantaneous frequency (IF) of the contaminated clutter will vary from pulse-to-pulse, and thus broadening the clutter spectrum. This can be corrected if the IF is compensated to be a fixed value.

In general, the ionosphere instability is modeled by a multiplicative noise [6]. This causes the Bragg frequency shifts around the theoretical value. The key idea of the compensation scheme is to find the IF of the Bragg line. Several algorithms have been proposed. Bourdlillon et al. [7] used maximum entropy spectral analysis algorithm to compensate the clutter. In this algorithm, one coherent processing interval (CPI) is divided into several short segments, during a short segment the Bragg frequency is regarded as stable. Within each segment, the frequency is estimated by high-resolution spectral analysis algorithm. This method performs well in slow perturbations, but if the frequency is not stable in the short duration or fast moving, its performance can be degraded. Parent and Bourdlillon [8] presented a simple energy-weighted phase differential estimator to track the IF of the contamination. This estimator requires a more complex transmission waveform and is not suitable to conventional FMCW radar systems. Khan [1] proposed an algorithm to suppress the clutter based on AR model. It got a good result to make the target clearly shown after clutter removed. The contamination was not considered. Howland and Cooper [9] used the Wigner–Ville distribution (WVD) to estimate the IF. WVD method is a two-dimensional computation. Moreover, due to limited data samples are used on both sides, the estimation on two edges is very coarse. As the compensation performance is determined by the accuracy of the frequency estimation, so the estimated frequency on both sides often should be discarded in order not to degrade its performance.

Poon et al. [10] proposed to suppress the clutter based on Hankel rank reduction (HRR) method. Lu et al. [11] proposed an improvement to HRR algorithm. In their study, they proposed to compensate the clutter using the IF shift and thus achieved a better performance in suppressing the clutter. The HRR can be used to estimate the IF of superimposed sinusoidal signals, but its performance decreases dramatically when the IF changes fast. Peleg and Friedlander [12] modeled the phase perturbation using a polynomial phase with constant magnitude. Then the higher-order phases are peeled-off order by order. Lu et al. [13] used this algorithm to compensate the skywave clutter. The problem for this algorithm is that there is no basic rule on how to determine the order for the polynomial phase. The order plays a key role in the performance of this algorithm.

In this article, a novel decontamination algorithm based on the complex energy detector (CED) is proposed. The energy detector (ED) was originally proposed for demodulating the AM–FM-modulated signals [14]. Bovik et al. [15] proposed to improve its performance by analytic wavelet transform (see, e.g., [16]). In this article, the detector is expanded for complex signals. I/Q orthogonal process is often used in radar environment. With this expansion, there will be no mutual coupling between the magnitude and frequency component for one signal. As in this application, only the frequency component is of concern.

The output of the CED operator is the square of the IF of one signal, IF can be derived directly via this detector by calculating its square root. Comparing with some other decontamination methods, CED is easy to implement. The algorithm is based on the complex AM–FM signal model, the impact of the magnitude is also considered. It can track larger frequency fluctuation than the HRR algorithm thus in this situation, it has better performance in compensating the contamination.

In this article, we consider the single-mode propagation model, which means that the Bragg components and the moving target in the same range cell are contaminated by the same function. This article is organized as follows. Section 2 introduces the ED and the CED method, and the principle on calculating the IF shift is explained. In Section 3, the clutter correction algorithm will be presented. Section 4 will give some simulation results to show its performance. And Section 5 concludes this article.

2. ED and CED

IF estimation plays a central role in the ionospheric clutter decontamination. In this section, the proposed CED algorithm is studied, and the scheme of the IF estimation based on CED is also explained. The ED was originally designed to demodulate the AM–FM-modulated signals. And for one real signal $s_r(t)$, its ED can be expressed as [14,15]

$$\psi(s_r) = (\dot{s}_r)^2 - (\ddot{S}_r)s_r \tag{2}$$

In the above equation, $\dot{s}_r$ and $\ddot{s}_r$ are the first- and second-order derivatives of signal s_r, respectively. It has been shown that if the real signal is AM–FM modulated, then the magnitude and frequency component can be derived by $\psi(s_r)$ and $\psi(\dot{s}_r)$. It is obviously that there is a coupling between the magnitude and frequency component. As in our application, only the frequency component is of concern. Moreover, in radar application environment, the signal is often processed by I/Q decomposition and in complex domain (see, for example [17]).

In this article, the CED is proposed to get rid of the issues mentioned above. For a complex signal, also AM–FM modulated, it can be expressed by

$$\begin{aligned} x(t) &= a(t)e^{j[2\pi f_b t + k\int_{-\infty}^{t} f(\tau)d_{\tau+\theta_0}]} \\ &= a(t)e^{j\theta(t)} \end{aligned} \tag{3}$$

where $a(t)$ is the instantaneous magnitude, $\theta(t)$ is its instantaneous phase, f_b is the carrier frequency, while k and $f(t)$ are the frequency modulation index and modulation signal, respectively. Let its first- and second-order derivates are $\dot{x}$ and $\ddot{x}$, respectively, then we have

$$\begin{cases} \dot{x} = \dot{a}e^{j\theta} + jae^{j\theta}\dot{\theta} \\ \ddot{x} = e^{j\theta}\left(\ddot{a} + 2j\dot{a}\dot{\theta} - a\left(\dot{\theta}\right)^2 + ja\ddot{\theta}\right) \end{cases} \tag{4}$$

If we define the CED for the complex signal s as

$$\psi(s) = |\dot{s}|^2 - (\ddot{s})^* s \tag{5}$$

where the * is the conjugate operator. Then, for the complex AM–FM-modulated signal x, we have

$$\begin{aligned} \psi(x) =& |\dot{x}|^2 - (\ddot{x})^* x \\ =& \left(\dot{a}e^{j\theta} + jae^{j\theta}\dot{\theta}\right)\left(\dot{a}e^{j\theta} + jae^{j\theta}\dot{\theta}\right)^* \\ & - e^{-j\theta}\left(\ddot{a} - 2j\dot{a}\dot{\theta} - j\ddot{\theta}a - a\left(\dot{\theta}\right)^2\right)ae^{j\theta} \\ =& \left(\dot{a} + ja\dot{\theta}\right)\left(\dot{a} - ja\dot{\theta}\right) \\ & - \left(\ddot{a} - 2j\dot{a}\dot{\theta} - j\ddot{\theta}a - a\left(\dot{\theta}\right)^2\right)a \\ =& (\dot{a})^2 + a^2\dot{\theta}^2 - \ddot{a}a + 2j\dot{a}a\dot{\theta} + j\ddot{\theta}a^2 + a^2\dot{\theta}^2 \\ =& \psi(a) + 2a^2\dot{\theta}^2 + 2j\dot{a}a\dot{\theta} + j\ddot{\theta}a^2 \end{aligned} \tag{6}$$

In order to derive $\dot{\theta}$, which is the IF of signal x, we get the real component in Equation (6), and then we have (note that $\psi(a)$ is already real)

$$\dot{\theta}^2 = [\mathrm{Re}\{\psi(x)\} - \psi(a)]/2a^2 \tag{7}$$

where a is the instantaneous magnitude of the complex signal x, $\psi(a)$ the CED of the signal magnitude which can be computed by Equation (5).

For the reason of simplicity, time index t is omitted. From Equation (7), it is found that, by applying the CED to the AM–FM signal, the first-order derivate of the phase signal can be derived directly. From Equation (3), $\dot{\theta}$ is the sum of $2\pi f_b$ and linear scalar of the $f(t)$. So, $f(t)$ can be recovered using Equation (7). Once $f(t)$ is demodulated, it can be used to compensate the phase shift caused by the ionosphere. This is the idea of the CED. It should be noted that after a squaring root operation of Equation (7), the actual IF of the Bragg component is derived. Theoretically, the frequency shift caused by the ionosphere can be obtained by subtracting the Bragg frequency $2\pi f_b$. But, considering the ocean current velocity, as it will cause a frequency shift to the first-order peak proportional to its velocity [18], $2\pi f_b$ is replaced by the average value of the actual IF.

Except the multiplicative noise in the ocean clutter return, the additive noise is also worthy of analysis. The former type of noise will smear the spectrum, while the latter one will raise the clutter level and also decreases the probability of detection of the target. Suppose that a complex noise $\nu(t)$ is added in the clutter signal. It can be expressed as

$$\nu(t) = \nu_1(t) + j\nu_2(t) \tag{8}$$

where $\nu_1(t)$ and $\nu_2(t)$ are both wide-sense-stationary (WSS) zero-mean real Gaussian processes. They are statistically independent of each other, and also independent of the clutter signal. They have the same first- and second-order moments. The autocorrelation is $R_{\nu_1}(\tau)$ and with variance σ_n^2. Let the signal with additive noise be $s(t) = x(t) + \nu(t)$, then apply the CED to signal $s(t)$, we have

$$\begin{aligned} \psi(s) =& |\dot{s}|^2 - (\ddot{s})^* s \\ =& (\dot{x} + \dot{\nu})(\dot{x} + \dot{\nu})^* - (\ddot{x} + \ddot{\nu})^*(x + \nu) \\ =& |\dot{x}|^2 + \dot{x}(\dot{\nu})^* + \dot{\nu}(\dot{x})^* + |\dot{\nu}|2 - (\ddot{x})^* x - (\ddot{x})^*\nu - (\ddot{\nu})^* x - (\ddot{\nu})^*\nu \\ =& (|\dot{x}|^2 - (\ddot{x})^* x) + (|\dot{\nu}|^2 - (\ddot{\nu})^*\nu) + (\dot{x}(\dot{\nu})^* \\ & + \dot{\nu}(\dot{x})^* - (\ddot{x})^*\nu - (\ddot{\nu})^* x) \\ =& \psi(x) + \psi(\nu) + (\dot{x}(\dot{\nu})^* + \dot{\nu}(\dot{x})^* - (\ddot{x})^*\nu - (\ddot{\nu})^* x) \end{aligned} \tag{9}$$

It shows that, if one signal is perturbed by an additive noise, then its CED is the sum of the signal and noise plus some cross terms. In the equation, only $\psi(x)$ should be used to estimate the frequency, all other terms are regarded as noise. So, it is necessary to analysis the impact of these terms, i.e.

$$\psi(s) - \psi(x) = \psi(\nu) + (\dot{x}(\dot{\nu})^* + \dot{\nu}(\dot{x})^* - (\ddot{x})^*\nu - (\ddot{\nu})^* x) \tag{10}$$

For a real WSS stochastic process $y(t)$, its first- and second-order derivatives are both WSS. $\dot{y}(t)$ is statistically independent of $\ddot{y}(t)$ and $y(t)$. It has been proved that [19]

$$R_{\dot{y}\dot{y}}(\tau) = -\ddot{R}_{yy}(\tau) \tag{11}$$

Apply Equation (11) to the complex noise $\nu(t)$, we have

$$E[|\dot{\nu}|^2] = E[|\dot{\nu}_1|^2+|\dot{\nu}_2|^2] = -2\ddot{R}_{\nu_1}(0) \tag{12}$$

$$E[(\ddot{\nu})^*\nu] = E[(\ddot{\nu}_1 + j\ddot{\nu}_2)^*(\nu_1 + j\nu_2)] = E[\ddot{\nu}_1\nu_1] + E[\ddot{\nu}_2\nu_2] = 2\ddot{R}_{\nu_1}(0) \tag{13}$$

Combining Equations (12) and (13), the mean of $\psi(\nu)$ is

$$E[\psi(\nu)] = -4\ddot{R}_{\nu_1}(0) \tag{14}$$

For the last four terms in Equation (10), it can be shown that their mean are all zero. Then the expect value of $\psi(s) - \psi(x)$ is

$$E[\psi(s) - \psi(x)] = -4\ddot{R}_{\nu_1}(0) \tag{15}$$

From Equation (15), when additive noise is added into the clutter, $\psi(s)$ is a biased estimation of $\psi(x)$, with bias $-4\ddot{R}_{\nu_1}(0)$. Since the noise is added, then in Equation (7), the term x will be replaced by s, and a will be replaced by b, where b is the instantaneous magnitude of s. Let the estimated $\dot{\theta}^2$ be $\hat{\dot{\theta}}^2$, with the assumption of high clutter-to-noise ratio (CNR), the expected value can be approximated by

$$\begin{aligned} E\left[\hat{\dot{\theta}}^2\right] &= E[[\mathrm{Re}\{\psi(s)\} - \psi(b)]/2b^2] \\ &\approx \frac{E[\mathrm{Re}\{\psi(x)\} + \mathrm{Re}\{\psi(\nu)\} - \psi(b)]}{E[2b^2]} \\ &= \frac{2a^2\dot{\theta}^2 + \psi(a) + E[\mathrm{Re}\{\psi(\nu)\}] - E[\psi(b)]}{E[2b^2]} \\ &\approx \frac{2a^2\dot{\theta}^2 + E[\mathrm{Re}\{\psi(\nu)\}]}{E[2b^2]} \\ &= \frac{2a^2\dot{\theta}^2 - 4\ddot{R}_{\nu_1}(0)}{2\left(a^2 + 2\sigma_n^2\right)} \end{aligned} \tag{16}$$

where the following relations are used for the approximation

$$\psi(a) = \mathrm{E}[\psi(b)] \tag{17}$$

$$E\left[b^2\right] = a^2 + 2\sigma_n^2 \tag{18}$$

Equation (17) holds under the assumption of high CNR, while in Equation (18), the statistical property of the additive noise is used. The σ_n^2 is the variance of the real or equivalently the imaginary part of the additive complex noise.

For digital implementation, the derivatives can be expressed by the following approximations:

$$\dot{x}(n) = [x(n+1) - x(n)]/T \tag{19}$$

$$\begin{aligned} \ddot{x}(n) &= [\dot{x}(n+1) - \dot{x}(n)]/T \\ &= [x(n+2) - x(n+1)] - [x(n+1) - x(n)]/T^2 \\ &= [x(n+2) - 2x(n+1) + x(n)]/T^2 \end{aligned} \tag{20}$$

Substituting Equations (19) and (20) into Equation (6), we have

$$\begin{aligned} \psi(x(n)) &= |[x(n+1) - x(n)]/T|2 \\ &\quad - ([x(n+2) - 2x(n+1) + x(n)]/T^2)^*x(n) \\ &= [|x(n+1)|^2 - x(n+1)x^*(n) \\ &\quad -x(n+2)^*x(n) + x^*(n+1)x(n)]/T^2 \end{aligned} \tag{21}$$

3. The decontamination algorithm based on CED

The idea of compensating the ionosphere movement is to track the IF movement of the Bragg frequency. According to Equation (7), if we apply the CED to one Bragg frequency component, then the IF $\dot{\theta}$ of the signal can be found

$$\dot{\theta} = \pm\sqrt{[\mathrm{Re}\{\psi(x)\} - \psi(a)]/2a^2} \tag{22}$$

From this formula, the frequency modulation component $f(t)$ can be derived by simply computing its square root. This formula will be applied to one of the strongest Bragg component, which will be explained next. The sign of Equation (22) depends on which Bragg component we choose for processing. Once $f(t)$ is computed, the contamination can be compensated accordingly. The compensation is achieved by multiplying the conjugate of the frequency-modulated component, as

$$s_c = se^{-jk\int_{-\infty}^{t} f(\tau)d\tau} \tag{23}$$

With this compensation, the Bragg peak will be sharper and target can be discriminated. Figure 1 shows the decontamination algorithm based on the CED, and it is descried as follows

(1) For the data of one cell in a CPI, perform FFT, and transform it into frequency domain.
(2) Search the strongest peak at the range of $[-5f_b, 5f_b]$, where f_b is the theoretical Bragg frequency.

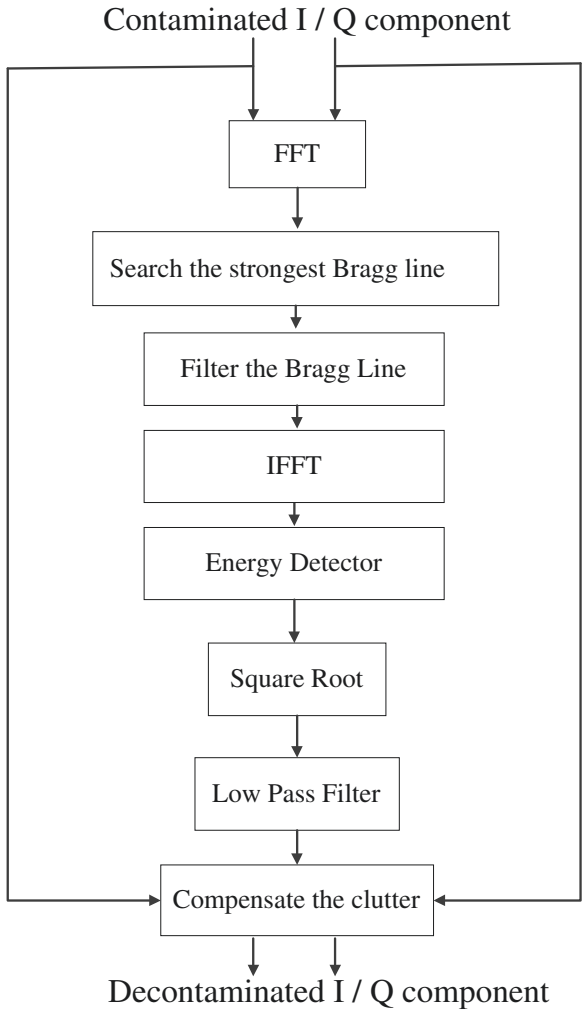

Figure 1 Compensation procedure based on the CED.

(3) Filter out the strongest Bragg peak, or equivalently, mask other frequency bin. This Bragg peak will be used for estimating the IF.
(4) Transform the filtered data into time domain via IFFT.
(5) Perform CED to the Bragg component.
(6) Compute the square root of the CED, and extract the frequency modulation component.
(7) Apply a low pass filter to the result of step 6 to reduce the ripple due to differentiation.
(8) Compensate the clutter using Equation (23), get the "clean" version of the clutter.

Table 1 Simulation parameters

A_1	A_2	f_b	f_t	B	$k1/k2$
5	7	0.32	0.52 Hz	0.6	0/0.2
f_{m1}	T	f_c	CNR	SNR	N
0.2/0.1 Hz	0.1 s	10 MHz	25 dB	5 dB	256

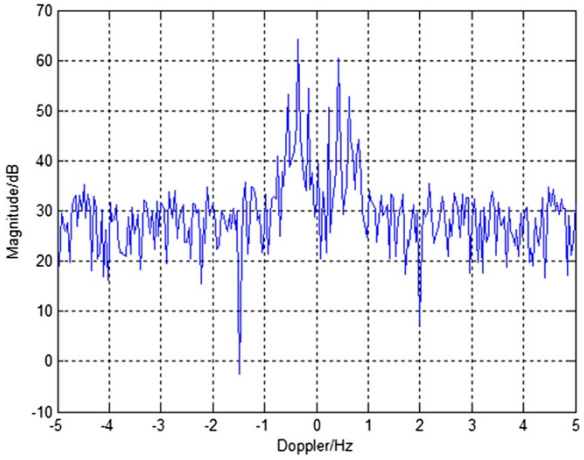

Figure 2 The contaminated return signal (f_{m1} = 0.2, B = 0.6).

In step (3), a rectangular window in frequency domain is used to extract strongest Bragg component. The bandwidth of this filter is an important factor to be considered. The basic rule for choosing this parameter is to retain most of the contamination component while reject other unwanted ones. On the one hand, if it is too wide, then part of the second-order spectrum and more noise will be included. This will impact the performance of the CED algorithm. On the other hand, if it is too narrow, the contamination of one Bragg component may not be fully covered. Howland and Cooper [9] suggested the bandwidth to be 0.5 Hz as a typical value.

In the following section, some simulation results will be presented to show the performance of the CED algorithm. The result of CED algorithm will be compared with formerly proposed HRR algorithm.

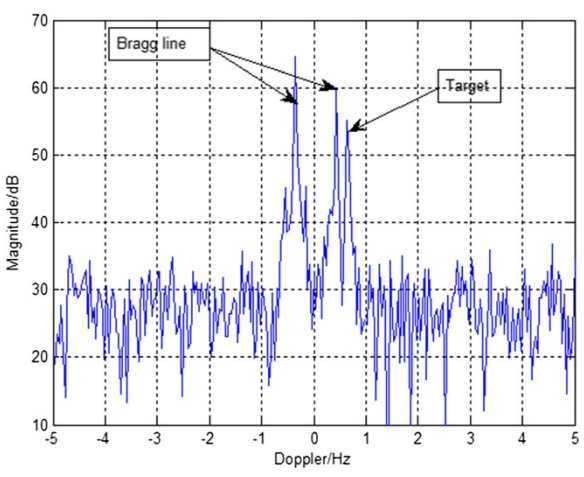

Figure 3 The decontaminated return signal (f_{m1} = 0.2, B = 0.6).

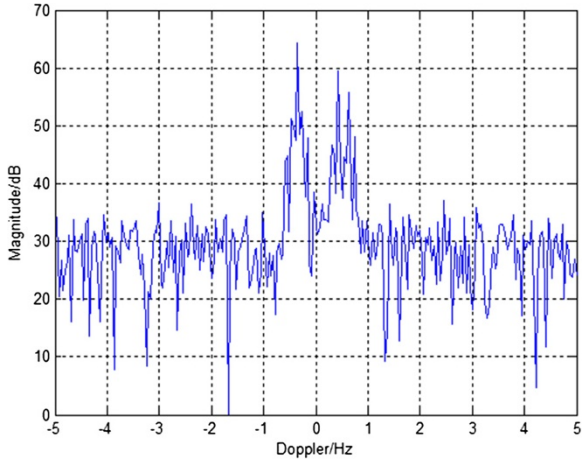

Figure 4 The contaminated return signal (f_{m1} = 0.1, B = 0.6).

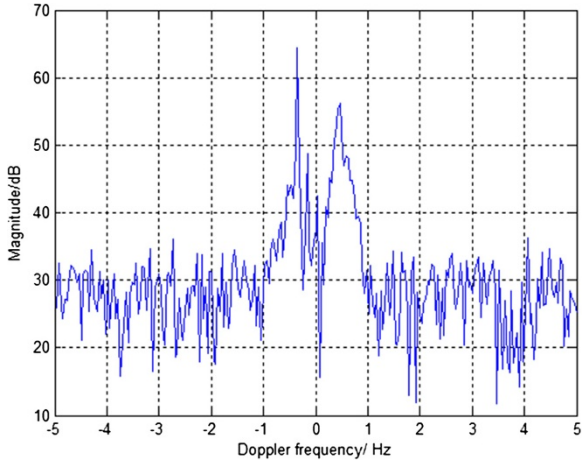

Figure 6 The decontamination result of the HRR algorithm (f_{m1} = 0.2, B = 0.6).

4. Simulation results

In this section, the simulation results will be presented. The signal model used in this article is

$$\begin{cases} s(t) = s_1(t) + s_2(t) + s_t(t)e^{j\phi(t)} + v(t) \\ s_1(t) = A_1(1 + k_1x_1(t))e^{j(2\pi fbt + B\cos(2\pi f_{m1}t + \theta_1))} \\ s_2(t) = A_2(1 + k_2x_2(t))e^{j(-2\pi f_bt + B\cos(2\pi f_{m1}t + \theta_1))} \end{cases} \tag{24}$$

where $s_1(t)$ and $s_2(t)$ are two Bragg clutter components, which we suppose that they have the same contamination function or frequency fluctuation. The two signals $x_1(t)$ and $x_2(t)$ are both monochromatic signals with normalized magnitude and the frequency is 0.2 Hz. The term $st(t)$ is the target signal. It is modeled by a monochromatic signal with Doppler frequency f_t. The term $\phi(t)$ is the contamination function which is caused by the ionosphere. In the simulation, we assume that it is single-mode propagation so that the target signal experiences the same frequency perturbation as the Bragg clutter components. The T is the sampling period, N data samples are processed in one CPI. For the contamination function, the parameter B characterizes the fluctuation magnitude of the phase, a larger B means larger fluctuation, and vice versa. While f_{m1} characterizes the fluctuation rate of the phase, the phase changes faster with larger values. And $v(t)$ is the additive white Gaussian noise. The CNR is defined as the ratio of the two Bragg components to the additive noise, while signal-to-noise ratio (SNR) is the ratio of the moving target to the additive noise. The simulation parameters are shown in Table 1 for clear view.

Figures 2, 3, 4, and 5 show a series of simulation results with f_{m1} varies accordingly. The parameter B is the

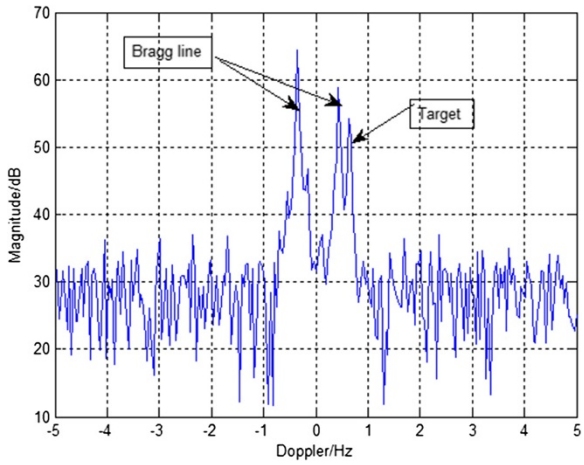

Figure 5 The decontaminated return signal (f_{m1} = 0.12, B = 0.6).

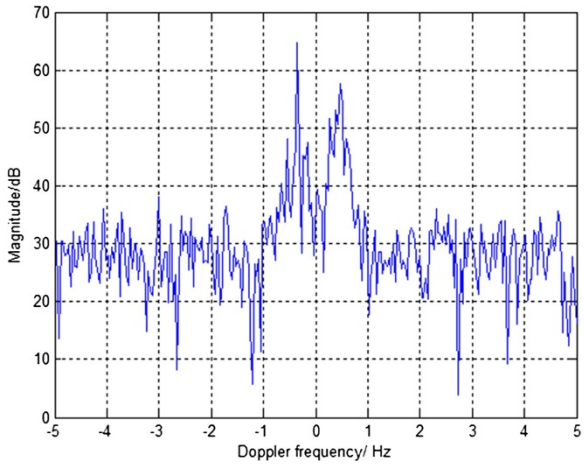

Figure 7 The decontamination result of the HRR algorithm (f_{m1} = 0.1, B = 0.6).

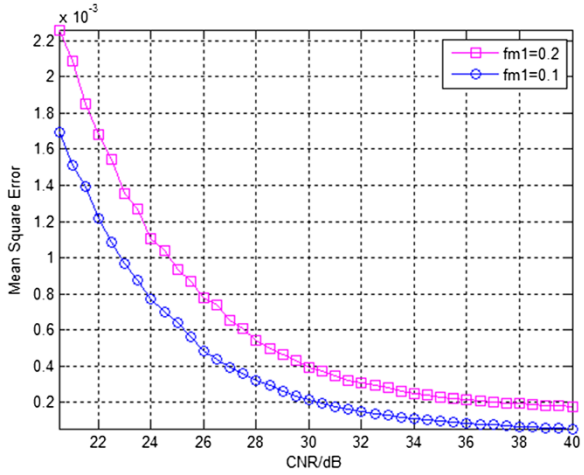

Figure 8 MSE of the CED algorithm.

magnitude of the contamination function. In the simulation, we use large B to show that the CED algorithm can track larger frequency fluctuations with specified parameters than the HRR algorithm. Figures 2 and 3 show the result when f_{m1} =0.2, B = 0.6. In which, Figure 2 shows the contaminated radar return signal, Figure 3 shows the decontaminated return signal by using the CED algorithm. In the figure, we can see that, after the compensation, both of the Bragg peaks and target are much sharper. The target now is easily to be discriminated, while in the contaminated data of Figure 2, the target is buried.

Figures 4 and 5 show the result when f_{m1} = 0.1, B = 0.6. In which, Figure 4 shows the contaminated data, Figure 5 shows the decontaminated return signal by using the CED algorithm. In the figure, we can also see that, after the compensation, both of the Bragg peaks and target are much sharper. The target can be discriminated, while in the contaminated data of Figure 4, the target is buried.

Figures 6 and 7 show the corresponding decontamination results of the HRR algorithm, where Figure 6 shows the compensated spectrum when f_{m1} = 0.2 and B = 0.6, by using the simulated data of Figure 2. Figure 7 shows the compensated spectrum of f_{m1} = 0.1 and B = 0.6 by using the simulated of Figure 4. From the compensated clutter shown in Figures 6 and 7, the CED algorithm can outperform the HRR algorithm under the specified simulation parameter setting. In HRR, the target cannot be detected clearly after compensated, while the Bragg lines are still broad with glitches and high side lobes. For the computational time, in one realization, 0.093 s is cost for one range cell data by the CED algorithm, while the HRR algorithm consumes 0.063 s. The algorithm can be implemented in real time.

Figure 8 shows the mean square error (MSE) of the IF estimation using the parameters in Table 1 but with the CNR varies from 20 to 40 dB. The upper line shows the MSE for f_{m1} = 0.2, and the lower line shows the MSE for f_{m1} = 0.1. It can be seen that the MSE decreases monotonically and converges with the CNR.

By analyzing the simulation results, we conclude that the CED algorithm-based compensation can work and outperform HRR algorithm in large frequency perturbations. As in this situation the HRR algorithm will fail to track the IF change thus it degrades the compensation performance.

5. Conclusions

In this article, a novel skywave OTH radar ocean clutter decontamination algorithm based on the CED is proposed. The ED was originally designed to demodulate the AM–FM-modulated signals. In this article, it is expanded to complex domain. With this expansion, the frequency shift of the clutter can be derived directly by computing the root square of CED for one complex signal. The clutter is then corrected by using the IF shift estimated by the CED algorithm. The procedure of algorithm is presented clearly. Simulation results are also presented. Simulation results suggest that the CED algorithm can be used to compensate the clutter frequency fluctuation due to ionosphere instability or movement. Its result is better than HRR algorithm in large perturbations. It is also easy to implement with proper computational complexity.

Competing interests

The authors declare that they have no competing interests.

Acknowledgements

This study was supported by the National Science Foundation of China under Grant 61032010, and by the NSAF under Grant 11076006. The authors would like to thank the anonymous reviewers for their constructive comments and suggestions helped in improving the quality and presentation of this article.

Received: 21 March 2012 Accepted: 18 October 2012
Published: 26 November 2012

References

1. RH Khan, Ocean-clutter model for high-frequency radar. IEEE J. Ocean Eng. **16**(2), 181–188 (1991)
2. GJ Frazer, YI Abramovich, BA Johnson, Multiple-input multiple-output over-the-horizon radar: experimental results. IET Radar Sonar Navigat. **3**(4), 290–303 (2009)
3. A Capria, F Berizzi, R Soleti, ED Mese, A frequency selection method for HF-OTH skywave radar systems, in *Proc. of the EUSIPCO 2006 Conference* (Florence, 2006)
4. GF Earl, BD Ward, Frequency management support for remote sea-state sensing using the Jindalee skywave radar. IEEE J. Ocean Eng. **11**(2), 164–172 (1986)
5. V Bazin, JP Molinie, J Munoz, P Dorey, S Saillant, G Auffray, V Rannou, M Lesturgie, NOSTRADAMUS: an OTH radar. IEEE Aerosp. Electron. Syst. Mag. **21**(10), 3–11 (2006)
6. YI Abramovich, SJ Anderson, ISD Solomon, Adaptive ionospheric distortion correction techniques for HF skywave radar, in *Proc. 1996 IEEE Nat. Radar Conf* (, Michigan, 1996), pp. 267–272

7. A Bourdlillon, F Gauthier, J Parent, Use of maximum entropy spectral analysis to improve ship detection over-the-horizon radar. Radio Sci. **22**(2), 313–320 (1987)
8. J Parent, A Bourdlillon, A method to correct HF skywave backscattered signals for ionospheric frequency modulation. IEEE Trans. Antennas Propagat. **36**(1), 127–135 (1988)
9. PE Howland, DC Cooper, Use of the Wigner–Ville distribution to compensate for ionospheric layer movement in high-frequency sky-wave radar systems. IEE Proc. F: Radar Signal Process. **140**(1), 29–36 (1993)
10. MWY Poon, RH Khan, S Le-Ngoc, A singular value decomposition (SVD) based method for suppressing ocean clutter in high frequency radar. IEEE Trans. Signal Process. **41**(3), 1421–1425 (1993)
11. K Lu, XZ Liu, YT Liu, Ionospheric decontamination and sea clutter suppression for HF skywave radars. IEEE J. Ocean Eng. **30**(2), 455–462 (2005)
12. S. Peleg, B. Friedlander, The discrete polynomial-phase transform. IEEE Trans. Signal Process. **43**(8), 1901–1914 (1995)
13. K Lu, J Wang, XZ Liu, A piecewise parametric method based on polynomial phase model to compensate ionospheric phase contamination, in *Proc. ICASSP 2003*, 2nd edn. (, Hong Kong, 2003), pp. 406–409
14. P Maragos, JF Kaiser, TF Quatieri, On amplitude and frequency demodulation using energy operators. IEEE Trans. Signal Process. **41**(4), 1532–1550 (1993)
15. AC Bovik, P Maragos, TF Quatieri, AM-FM energy detection and separation in noise using multiband energy operators. IEEE Trans. Signal Process. **41** (12), 3245–3265 (1993)
16. S Mallat, *A Wavelet Tour of Signal Processing—The Sparse Way*, 3rd edn. (Academic Press, Orlando, 2008), pp. 89–149
17. G Fabrizio, F Colone, P Lombardo, A Farina, Adaptive beamforming for high-frequency over-the-horizon passive radar. IET Radar Sonar Navigat. **3**(4), 384–405 (2009)
18. BJ Lipa, DE Barrick, Extraction of sea state from HF radar sea echo: mathematical theory and modeling. Radio Sci. **21**(1), 81–100 (1986)
19. A Papoulis, *Probability, Random Variables, and Stochastic Process*, 2nd edn. (, McGraw-Hill, 1984)

doi:10.1186/1687-6180-2012-246
Cite this article as: Wei *et al.*: Ionospheric decontamination for skywave OTH radar based on complex energy detector. *EURASIP Journal on Advances in Signal Processing* 2012 **2012**:246.